Colloquia: Channeling 2010

Bremsstrahlung from relativistic bare heavy ions in single crystals

A. H. Sørensen(*) and T. V. Jensen

Department of Physics and Astronomy, University of Aarhus - DK-8000 Aarhus C, Denmark

Summary. — We calculate the bremsstrahlung emitted by heavy bare ions penetrating single crystals at highly relativistic energies. The main component, originating in scattering of the virtual photons of screened target nuclei on the projectile, appears with energies of, approximately, 25γ MeV for a lead ion ($\gamma \equiv E/Mc^2$ where E and M denote projectile energy and mass). It shows dips in yield upon variation of the incidence angle to major crystallographic directions quite similar to those of other close-encounter processes. Incoherent interaction with single target electrons gives rise to two additional but quite different bremsstrahlung components, a moderate component distributed over the same frequencies as the main component, and a strong component confined to low energies. The channeling characteristics of the total bremsstrahlung spectrum vary substantially with photon energy.

PACS 41.60.-m – Radiation by moving charges.
PACS 61.85.+p – Channeling phenomena (blocking, energy loss, etc.).

1. – Introduction

Formulas and remarks in the literature have suggested that bremsstrahlung is the major source of energy loss for heavy ions at sufficiently high energies exactly as for electrons [1,2]. We have previously proven this not to be true [3]. Below a brief account is given of the various contributions to heavy-ion bremsstrahlung, including three not shown before. The expected spectrum is displayed. We continue with examination of the emission for cases where the target is a single crystal rather than an amorphous substance.

2. – Channeling radiation

Let us start out by checking the characteristics of channeling radiation well known for electrons and positrons. Our favorite projectile ion is a bare ^{208}Pb-nucleus (atomic

---

(*) E-mail: ahs@phys.au.dk

number $Z = 82$). Let us assume incidence at $\gamma = 170$, which is currently attainable at CERN, on a silicon single crystal (atomic number $Z_t = 14$) near the $\langle 111 \rangle$ axis (atomic spacing $d = 4.70\,\text{Å}$ along axis). In this situation the Lindhard (or critical channeling) angle ψ_1 [4], conveniently expressed in terms of the product of projectile momentum p and speed v [5,6], is much smaller than $1/\gamma$,

$$
(1) \qquad\qquad \psi_1 \equiv \left(\frac{4ZZ_t e^2}{pvd} \right)^{1/2} \ll 1/\gamma
$$

($\gamma\psi_1 = 3.5 \times 10^{-3}$). This implies: i) the motion in the frame $\mathcal{R}$ following the projectile (on average), the so-called rest frame, is non-relativistic, and ii) we are far from the region where the "constant field" (or "synchrotron") approximation may be applied since the changes in direction are much smaller than the opening angle of the light cone. Characteristic energies for coherent radiation associated with channeling or near-channeling motion may then be estimated by simple means:

In the laboratory a periodicity $d_\perp$ in transverse space translates, for a projectile moving at an angle ψ to the considered crystallographic direction, to a frequency in the transverse motion of $\omega_d \sim 2\pi c\psi/d_\perp$ since the time between successive encounters with atomic rows or planes in the crystal is of order $(d_\perp/\psi)/c$, when v is close to c, the speed of light. If we take $d_\perp \sim 2\,\text{Å}$ and $\psi \sim \psi_1$ the estimate becomes $\hbar\omega_d \sim 2\pi\,\text{keV} \times \psi_1$. Due to time dilation the frequency in the motion encountered in $\mathcal{R}$ is a factor of γ higher, $\omega_d^{\mathrm{R}} = \gamma\omega_d$. Since the motion in $\mathcal{R}$ is non-relativistic the frequency characterizing the motion also characterizes the radiation emitted in this frame. A transformation back to the laboratory gives an extra factor of 2γ for forward emission, that is, we end up with radiation at, typically, $\omega \sim 2\gamma^2\omega_d$. The transformation also reveals that typical emission angles are of order $1/\gamma$. In the considered case $\psi_1 = 21\,\mu\text{rad}$ and we end up with an estimate of $\hbar\omega \sim 2\gamma^2\hbar\omega_d \sim 7.5\,\text{keV}$. Note that since ψ_1 scales as $1/\gamma^{1/2}$, the characteristic energy scales as $\gamma^{3/2}$.

The energies characteristic of channeling radiation are way below those characteristic for bremsstrahlung emitted in collisions with individual atoms: as we shall see below, the main peak in the spectrum of the latter scales with γ and, in the considered case, appears about six orders of magnitude higher than our estimate for the former. In consequence, if we do not care about very low photon energies (or exceedingly high values of γ), we may forget about channeling radiation and channeling will show up solely "the old-fashioned way", that is, as a focusing effect. Hence, in the following we turn our attention to what in the field of channeling is known as incoherent bremsstrahlung. Actually, as we shall discuss shortly, coherence is also a key word in the emission of bremsstrahlung in collisions of heavy ions with individual atoms—the agents concerned are just acting on the nuclear rather than the atomic scale.

3. – Bremsstrahlung—procedure of calculation

When a bare heavy ion interacts with target constituents it generally emits electromagnetic radiation regardless of the final state of the projectile. However, when we speak about bremsstrahlung we shall restrict to cases where the projectile remains intact throughout the interaction. This restricts our attention to non-contact collisions, that is, to impact parameters between projectile and target nucleus in excess of the sum of the nuclear radii, $b > R + R_t \equiv R_\Sigma$ (target identified by subscript t). The condition $b > R_\Sigma$ is

not sufficient to guarantee no break-up. For instance, the probability for electromagnetic dissociation is high near R_Σ for heavy targets [7]. This may be corrected for; we shall not discuss such corrections further in this contribution.

The bremsstrahlung emitted by a bare heavy-ion penetrating matter is conveniently calculated by means of the Weizsäcker-Williams (WW) method of virtual photons since i) the electromagnetic field of a highly relativistic charge is nearly transverse to the direction of motion and has the shape of a suitable "equivalent" pulse of radiation and ii) cross-sections for photon scattering are extractable from the literature. There are four contributions to the bremsstrahlung when a bare heavy ion collides with a target atom corresponding to the possible combinations of virtual photon source and scatterer:

– screened target nucleus (WW) on projectile in the rest frame $\mathcal{R}$ of the latter

– projectile (WW) on target nucleus,

– projectile (WW) on individual target electrons,

– individual target electrons (WW) on projectile in $\mathcal{R}$.

As may be expected, *e.g.*, from studies of bremsstrahlung in electron-electron collisions [8], the first process listed gives the main contribution.

For a particle of charge q moving at constant speed $v = \beta c$ the energy transmitted per unit area and frequency ω by virtual photons at a transverse distance b from the particle path amounts to [9]

$$(2) \qquad \frac{\mathrm{d}I}{\mathrm{d}\omega \mathrm{d}^2 b} = \frac{q^2}{\pi^2 c \beta^2 b^2}[x K_1(x)]^2,$$

where K_1 is a modified Bessel function. The count spectrum (number of WW photons) results upon division by $\hbar\omega$. For a bare charged particle x is given as $x = \omega b/\gamma\beta c$, where the Lorentz factor relates to β as $\gamma = 1/\sqrt{1-\beta^2}$. The expression (2) holds also for a dressed particle of central charge q producing an exponentially screened Coulomb potential (Yukawa) in its rest frame; in this case x takes the more general form

$$(3) \qquad x = \sqrt{(\omega b/\gamma\beta c)^2 + (b/a)^2},$$

where a is the screening length [3]. Since K_1 falls off exponentially for arguments larger than 1, the effective range in ω for given b, or in b at given ω, is determined by the condition $x = 1$. For a screened source the range in impact parameter is obviously limited by the screening length. For incidence on an amorphous substance only the integral over impact parameter is of interest. Provided no additional b-dependent factors are included, *e.g.*, to account for depletion due to other processes, this integral may be performed analytically. The corresponding virtual photon intensity is given in [3].

4. – The main bremsstrahlung component

The main contribution to heavy-ion bremsstrahlung was considered in detail in [3]. Briefly, the factor multiplying $[x K_1(x)]^2$ in eq. (2) reduces to $\hbar\alpha Z_t^2/\pi^2 b^2$, where $\alpha = e^2/\hbar c$ is the fine-structure constant, and the expression (3) is applied for x with the Thomas-Fermi length $a_{\mathrm{TF}} = 0.885 a_0 Z_t^{-1/3}$ substituted for a ($\beta = 1$ where explicit,
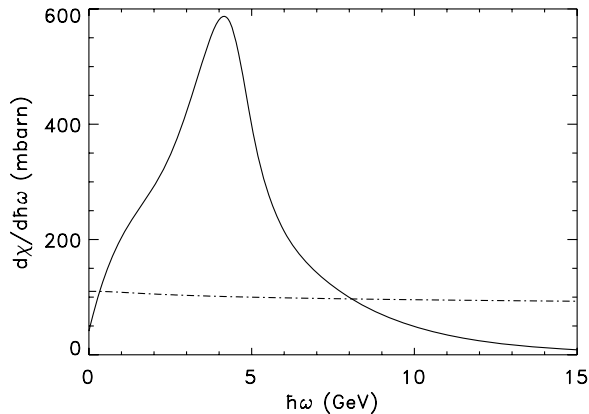
Fig. 1. – Main component of the bremsstrahlung spectrum for bare ^{208}Pb-ions penetrating a lead target at $\gamma = 170$. The chained curve displays the radiation cross-section for the hypothetical situation where both nuclei involved in a collision are pointlike and structureless.

a_0 is the Bohr radius of hydrogen). For the cross-section an expression differential in scattering angle is needed since the photon energy in the laboratory depends on the scattering angle in $\mathcal{R}$. The requirement of the projectile remaining intact translates into a requirement of coherent action of its constituents. Accordingly, the photon scattering separates roughly into three regimes: a) below $\hbar\omega_1$ (typical binding energy of a nucleon, roughly 8 MeV) scattering appears as on a point nucleus, b) beyond $\hbar\omega_1$ and up to $\hbar\omega_2 = \hbar c/R$ (wavelength equals nuclear radius, for ^{208}Pb about 28 MeV) the photon scatters coherently on Z quasifree protons, c) beyond $\hbar\omega_2$ incoherent scattering on single protons is possible. In the low-energy region (a) the Thomson cross-section pertaining to a point nucleus may be expected to apply approximately, in the intermediate region (b) the first guess is Z^2 times the Thomson cross-section for a single proton, but a resonance structure should be superimposed, in the high-energy region (c) fall-off is dictated by restriction to the coherent part of the scattering. Based on these observations we have created a fit [3] to the experimental data for elastic photon scattering on ^{208}Pb reported by Schelhaas *et al.* [10].

The product of the virtual photon intensity of the screened target nucleus in $\mathcal{R}$, integrated over impact parameters, and the elastic scattering cross-section produces the differential radiation intensity in $\mathcal{R}$ for an isolated target atom, that is, for an amorphous target. A transformation back to the laboratory gives the measurable spectra. Below, we shall display the "power spectra" or "radiation cross-sections" $\mathrm{d}\chi/\mathrm{d}\hbar\omega$ resulting after a final integration over emission angles.

Figure 1 displays the radiation cross section for bare lead ions penetrating an amorphous lead target at $\gamma = 170$. The structure of the projectile clearly reflects in the bremsstrahlung spectrum: the peak near 4 GeV reflects the resonance in the elastic scattering cross-section. Exactly as in channeling radiation, sect. **2**, the transformation from the rest frame to the laboratory results in a boost by a factor of $\simeq 2\gamma$. Beyond the peak the radiation cross section falls off quite fast due to the requirement of coherent action of the projectile constituents. The behavior is quite different from that which would result if both the projectile and the target nucleus were pointlike and structureless. In this
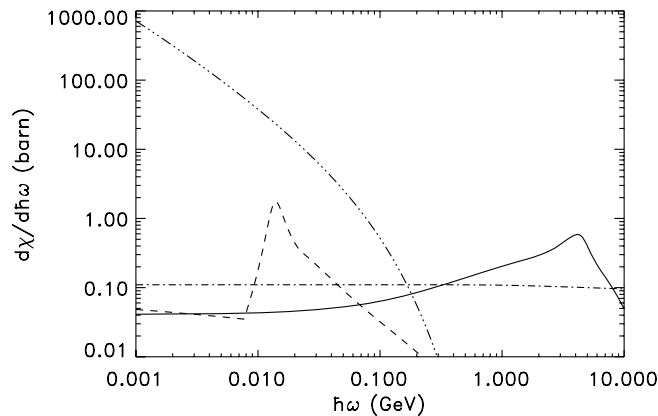
Fig. 2. – Bremsstrahlung due to scattering of the virtual photons of the projectile on target constituents for bare ^{208}Pb ions incident on lead at $\gamma = 170$. The component corresponding to scattering on target nuclei is shown by the dashed curve. The component corresponding to scattering on target electrons is shown by the triple-dot–dashed curve. The remaining curves are repeated from fig. 1.

case the radiation cross-section would be quite flat and featureless, the level would be considerably lower than the maximum in the actual situation, and the spectrum would extend essentially all way up to the impact kinetic energy. Exactly this last feature has led to the misconception of high bremsstrahlung losses mentioned in the introduction since the energy loss is proportional to the area under the curve. The height of the peak in the spectrum increases with γ but saturates at high values due to screening. An important feature not shown in the figure is that emission angles are of order $1/\gamma$. It follows from the Lorentz transformation combined with the fact that the scattering cross-section in $\mathcal{R}$ is not highly directional but Thomson-like where contributing most.

5. – The other contributions

5'1. – The scattering of virtual photons of the projectile on a target nucleus brings a relatively small amount of radiation at most energies: the contribution is only substantial for energies near the giant dipole resonance which is a factor of 2γ below the peak in the radiation spectrum deriving from the main bremsstrahlung component described above. Since no transformation between reference frames is involved, the contribution is obtained simply by multiplying the virtual photon intensity of the bare projectile by the total cross-section for elastic photon scattering at given ω. Figure 2 shows the result for the same collision system as in fig. 1. The photon scattering cross-section is obtained from the fit to the differential scattering cross-section by integration over angles.

5'2. – The scattering of virtual photons of the projectile on individual target electrons is standard Compton scattering (except perhaps for such low frequencies that atomic binding plays a role). In the Compton process the energy of the scattered photon is generally less than that of the incoming photon due to electron recoil. Hence, when we aim for the spectrum of radiated photons, the cross-section to multiply the virtual photon intensity of the projectile should be that for a photon of higher energy $\hbar\omega_0$ to scatter into a photon of the requested energy $\hbar\omega$ and an integration over all energies $\hbar\omega_0 > \hbar\omega$
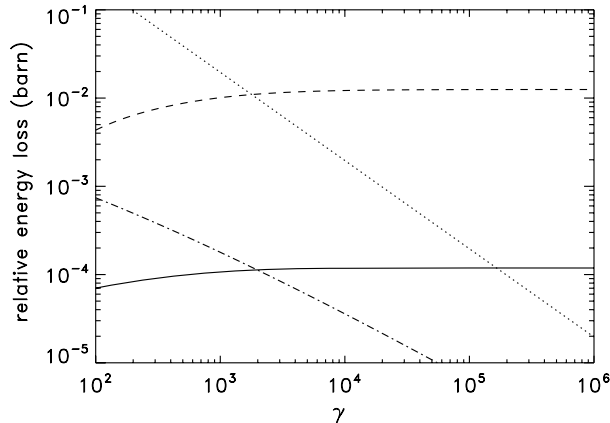
Fig. 3. – Relative energy loss of a bare lead ion penetrating a lead target. The full-drawn curve is the radiative loss due to the main bremsstrahlung component, the chained curve the Compton component of the radiative energy loss, the dotted curve the electronic energy loss, and the dashed curve the energy loss due to electron-positron pair creation. To get the fractional energy loss $-E^{-1}\mathrm{d}E/\mathrm{d}x$ per cm, the ordinate should be multiplied by 3.30×10^{-2}.

should be included. For the incoming spectrum the effective minimum impact parameter is half the Compton wavelength of the electron, $\hbar/2mc$, exactly as in the application of the WW method to the computation of bremsstrahlung for an electron in the field of an atomic nucleus [9]. This implies that the spectrum extends effectively up to a maximum of $\hbar\omega_0 \sim 2\gamma mc^2$. The latter is less than the peak in the main bremsstrahlung component by a factor of about 25 for the case of lead ions. Figure 2 includes a plot of the Compton component. Since the electrons are very effective scatterers due to their low mass, the radiation cross-section becomes high at low energies. The range of emission energies increases with γ but less fast than the main contribution. The characteristic photon-emission angle is inferable from the cross-section differential in scattering angle given by Heitler [8]. For photon energies well above mc^2 it amounts to $\sqrt{2mc^2/\hbar\omega_0}$ which reduces to $1/\sqrt{\gamma}$ at the effective maximum of the virtual photon spectrum.

The Compton processes add significantly to the energy loss at "moderate" values of γ. Figure 3 displays the radiative energy loss per unit path length, divided by the atomic density of the target, relative to the total impact energy $E = \gamma Mc^2$ as a function of γ. Losses due to atomic excitation and ionization [11] and electron-positron pair production [12] are also shown. Despite the Compton contribution, bremsstrahlung never dominates the energy loss of a bare heavy ion. Stopping is determined by electronic processes (lower γ) or pair production (higher γ).

$5^{.}3$. – The calculation of bremsstrahlung due to scattering of the virtual photons of a target electron on the projectile in the rest frame of the latter closely follows the calculation of the main bremsstrahlung component. There are two simple changes: i) Z_t^2 in the virtual photon spectrum is replaced by 1^2 and ii) the effective minimum impact parameter d is now the larger of the nuclear radius of the projectile and the de Broglie wavelength of the electron in $\mathcal{R}$ (for a lead projectile $d = R$ for, approximately, $\gamma > 55$).

Summing up the contributions from all Z_t electrons of a target atom results for the amorphous case in a bremsstrahlung component of essentially the same shape as the

main component but of relative magnitude $\sim 1/Z_t$. For a lead target this is only an additional $\sim 1\%$, for a silicon target the increase in yield is about 7%. For the crystalline case (rather, for non-uniform projectile flux in channels) the ratio of the electron to the nuclear component is obviously sensitive to the different location of target electrons and nuclei.

6. – Channeling dips

For the main bremsstrahlung component the source of virtual photons is the screened target nucleus. Hence the effective maximum impact parameter cannot exceed the screening length. For a silicon target the latter is only a few times the two-dimensional thermal vibration amplitude, $a_{\mathrm{TF}}/\rho = 2.5$ at $100\,\mathrm{K}$ for example. The entire impact-parameter range is orders of magnitude larger, for a lead projectile $a_{\mathrm{TF}}/R_\Sigma = 2.4 \times 10^3$. In consequence the main contribution to the heavy-ion bremsstrahlung appears essentially as a close-encounter process. Since the scattering cross-section has support effectively at limited energies, up to a few times $\hbar\omega_2$, screening will define the range at all photon energies at sufficiently high values of γ, cf. eq. (3) and remember that the effective maximum of x is ~ 1. This is the limit of "complete screening".

In the complete-screening limit, x appearing in eq. (2) reduces to b/a_{TF}. As a result, the dependence of the radiation cross-section on energy and impact parameter separates:

$$(4) \qquad \frac{\mathrm{d}\chi}{\mathrm{d}\hbar\omega\mathrm{d}^2b} = \frac{\mathrm{d}\chi}{\mathrm{d}\hbar\omega} \times \frac{1}{2\pi \ln(Ca_{\mathrm{TF}}/R_\Sigma)} \frac{1}{b^2} \left[\frac{b}{a_{\mathrm{TF}}} K_1\left(\frac{b}{a_{\mathrm{TF}}}\right) \right]^2 .$$

The first factor $\mathrm{d}\chi/\mathrm{d}\hbar\omega$ is the radiation spectrum obtained after integration over b (for the case with no depletion due to electromagnetic dissociation or similar). Accordingly, the second factor is normalized ($C = 0.681\ldots$ [3]).

Figure 4 shows the variation of the main bremsstrahlung component (dotted) with incidence angle in the complete-screening limit for a bare lead ion incident at a silicon single crystal near the $\langle 110 \rangle$ axis. The yield is normalized to that pertaining to amorphous silicon obtained upon incidence at angles to the axis much larger than the Lindhard angle ψ_1. The variation of the yield for a process requiring projectile and target nucleus to be at the same spot (δ-function interaction; "close-encounter process" in the standard channeling jargon) is also shown (dashed). The simplest possible channeling model is assumed (statistical equilibrium, no dechanneling), cf. [4-6]. Obviously the variation of the main bremsstrahlung component is not much different from that of a δ-function interaction. Since complete screening is assumed, the variation with angle is the same throughout the spectrum. At projectile energies below the complete-screening limit there will generally be a variation with photon energy. But regardless the values of ω and γ the variation is bound to stay between the two lower curves displayed in the figure.

The full-drawn curve in fig. 4 displays the variation when bremsstrahlung due to scattering of the virtual photons of the target electrons is included. This causes the dip to narrow and the minimum yield to increase. Both effects are due to the wider distribution of electrons than nuclei in the channel. While the target electrons only lead to an increase in the bremsstrahlung of 7% for "random" incidence (incidence far from major crystallographic directions corresponding to an amorphous medium), the minimum yield ($\psi = 0$) increases by a factor of 3.5 in fig. 4. Yet the overall behavior is still not so far from the result for "true close-encounter processes" (δ-function interaction).
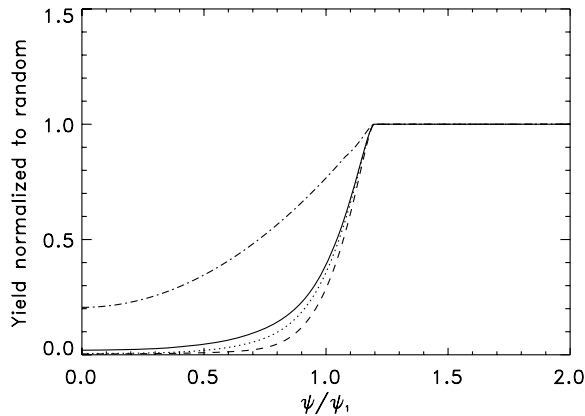
Fig. 4. – Axial channeling dips in bremsstrahlung for bare lead ions penetrating a silicon crystal cooled to 100 K. See text for explanation of curves.

The chained curve in fig. 4 shows the variation with incidence angle to the $\langle 110 \rangle$ axis of the upper end of the Compton component of the bremsstrahlung. Due to much wider distribution of electrons than nuclei in the channel the dip is much narrower and the minimum yield much higher than for the main component. Differences become even more pronounced if lower photon energies are selected. The different variations displayed in the figure imply substantial differences in the angular variation of the low- and the high-energy part of total bremsstrahlung spectra, that is, the shape of total bremsstrahlung spectra will change significantly with incidence angle under channeling conditions.

7. – Concluding remarks

Like bremsstrahlung, electron-positron pair production by relativistic bare heavy ions is essentially a close-encounter process in channeling context. However, since the minimum impact parameter is now of order the Compton wavelength of the electron, that is, about two orders of magnitude larger than the minimum impact parameter in the bremsstrahlung process, the impact-parameter range inside the thermal vibration amplitude of the crystal is somewhat less dominant. This implies that pair production has the potential of showing less pronounced channeling dips than bremsstrahlung. Actual differences turn out quite modest: for bare lead ions penetrating a silicon single crystal near the $\langle 110 \rangle$ axis at $\gamma = 170$ only the action of target electrons brings a slight deviation from the result for a δ-function interaction. If the projectile energy is raised corresponding to a γ-value of 3000 (LHC energy), the variation and values of the total yield appear not much different from those encountered for bremsstrahlung in the limit of complete screening, fig. 4; the nuclear contribution is slightly higher, the electron contribution slightly less, the sum about the same. The difference in the relative weight of the electronic contribution may be traced to a difference in threshold for the two pair-production components.

Above, as in [3], we have applied the Weizsäcker-Williams (WW) method. This is obviously not the only possibility for calculating heavy-ion bremsstrahlung. One alternative could be the formalism developed for so-called polarization bremsstrahlung, see, *e.g.*, [13]. The nuclear case is discussed in [14,15]. Note that the numerical results presented in the two last references pertain to nucleon impact on a nucleus with nuclear contact.

* * *

REFERENCES

[1] AHLEN S. P., *Rev. Mod. Phys.*, **52** (1980) 121.
[2] WEAVER B. A. and WESTPHAL A. J., *Nucl. Instrum. Methods B*, **187** (2002) 285.
[3] SØRENSEN A. H., *Phys. Rev. A*, **81** (2010) 022901.
[4] LINDHARD J., *K. Dan. Vidensk. Selsk., Mat. Fys. Medd.*, **34**, No. 14 (1965).
[5] SØRENSEN A. H. and UGGERHØJ E., *Nucl. Sci. Appl. A*, **3** (1989) 147.
[6] SØRENSEN A. H., *Nucl. Instrum. Methods Phys. Res. B*, **119** (1996) 1. Page 19 has been misplaced; it should be read after p. 16.
[7] BAGGESEN J. C. and SØRENSEN A. H., *Nucl. Instrum. Methods B*, **267** (2009) 2662.
[8] HEITLER W., *The Quantum Theory of Radiation*, 3rd ed. (Oxford University Press, London) 1954.
[9] JACKSON J. D., *Classical Electrodynamics*, 2nd ed. (Wiley, New York) 1975.
[10] SCHELHAAS K. P., HENNEBERG J. M., SANZONE-ARENHÖVEL M., WIELOCH-LAUFENBERG N., ZURMÜHL U., ZIEGLER B., SCHUMACHER M. and WOLF F., *Nucl. Phys. A*, **489** (1988) 189.
[11] LINDHARD J. and SØRENSEN A. H., *Phys. Rev. A*, **53** (1996) 2443.
[12] SØRENSEN A. H., *Nucl. Instrum. Methods B*, **230** (2005) 12. The full citation for ref. [2] in this paper is BELKACEM A. and SØRENSEN A. H., *Rad. Phys. Chem.*, **75** (2006) 656.
[13] KOROL A. V. and SOLOV'YOV A. V., *Rad. Phys. Chem.*, **75** (2006) 1266; 1251.
[14] AMUS'YA M. YA., GUL'KAROV I. S., ZHALOV M. B., POTAPOVA T. M., *Sov. J. Nucl. Phys.*, **40** (1984) 839.
[15] AMUSIA M. YA. and SOLOV'YOV A. V., in *Proceedings of the International Symposium on Modern Developments in Nuclear Physics, Novosibirsk, 1987*, edited by SUSHKOV O. P. (World Scientific, Singapore) 1988, p. 425.